

Projectile remnants in central peaks of lunar impact craters

Z. Yue^{1,2}, B. C. Johnson³, D. A. Minton², H. J. Melosh^{2,3*}, K. Di¹, W. Hu¹ and Y. Liu¹

The projectiles responsible for the formation of large impact craters are often assumed to melt or vaporize during the impact, so that only geochemical traces^{1,2} or small fragments^{3,4} remain in the final crater. In high-speed oblique impacts, some projectile material may survive⁵⁻⁷, but this material is scattered far down-range from the impact site. Unusual minerals, such as magnesium-rich spinel^{8,9} and olivine^{10,11}, observed in the central peaks of many lunar craters are therefore attributed to the excavation of layers below the lunar surface. Yet these minerals are abundant in many asteroids, meteorites and chondrules¹²⁻¹⁵. Here we use a numerical model to simulate the formation of impact craters and to trace the fate of the projectile material. We find that for vertical impact velocities below about 12 km s^{-1} , the projectile may both survive the impact and be swept back into the central peak of the final crater as it collapses, although it would be fragmented and strongly deformed. We conclude that some unusual minerals observed in the central peaks of many lunar impact craters could be exogenic in origin and may not be indigenous to the Moon.

We used the hydrocode iSALE to perform two-dimensional (2D) impact simulations at a variety of impact velocities, most at lower velocities than expected for Earth-impacting asteroids. We focused on a simulation of the 93-km-diameter Copernicus crater because of the reports of olivine¹⁰ and Mg-spinel¹⁶ in its central peaks, but our simulation also applies to the similar-size Theophilus crater in which exotic Mg-rich spinels have also been reported¹⁷ as well as to the smaller Tycho crater¹⁸. We assumed a 7-km-diameter dunite projectile impacting a two-layer target intended to simulate the nearside crust of the Moon. We approximate the lunar mantle as dunite and the lunar crust as granite. In our models we use a lunar crustal thickness of 30 km corresponding to the minimum lunar crustal thickness at the Apollo 12 and 14 landing sites, the nearest to Copernicus crater¹⁹. Figure 1 and 2 show that even with this minimum crustal thickness mantle material is not excavated. We varied the impact velocities from 6 to 16 km s^{-1} . Our results show that the maximum excavation depth in all cases is no more than 7 km, too shallow to reach the lunar mantle. This result agrees well with previous estimates of the maximum amount of stratigraphic uplift observed in terrestrial complex craters²⁰ as well as model estimates of the maximum depth of excavation²¹.

These computations show that, whereas most of the dunite projectile is vaporized and little remains in the crater at impact velocities above 14 km s^{-1} (Fig. 2), much of it survives the impact at velocities less than 12 km s^{-1} (Fig. 1a–c). This material is highly fractured and may be partly melted, but it is not vaporized and

so much of it remains in the crater. In small, simple craters this material is dispersed in the ejecta and over the transient crater floor, as seen in the pre-collapse phases of our computer simulations (Fig. 1a). It eventually mixes into the breccia lens filling the final crater. However, during the formation of central peaks in complex craters, the initially dispersed projectile material is swept back together during the collapse so that most (but not all) of any surviving projectile material accumulates in the central peak region; some projectile material is also ejected and mixed with target material in the crater rim and proximal ejecta blanket. Underlying crustal material, which is inherently less refractory than the olivine in the projectile, is also fractured and melted within the crater, consistent with the inference that impact melt mantles the floor of Copernicus and forms ponds among the slump terraces and on the proximal ejecta blanket. However, none of the simulations indicated excavation of the underlying mantle. The results of our computations lead to the possibility that the olivine observed in the central peaks of Copernicus and other lunar craters may be a remnant of the projectile and thus does not indicate deep excavation of the lunar mantle or lower crust. In contrast to craters on the Earth or other large bodies, central peaks in lunar craters may exhibit exotic compositions that reflect the impactor, not target rocks excavated from below.

The results presented in Fig. 1a–c are from an axially symmetric 2D computation in which the impact angle is vertical. However, real impacts occur at a wide variety of angles²², the most probable of which is 45° , and one can ask whether the same projectile concentration will occur for such oblique impacts. Study of the size and position of central peaks in Venusian impact craters demonstrates that the form and position of central peaks in large craters bears no relation to the impact angle or direction, even for highly oblique impact craters²³. These results imply that the crater collapse process is not strongly affected by the angle of impact and that the same concentration mechanism delineated by 2D computations is applicable to oblique impacts. Although more of the projectile is expected to survive in highly oblique impacts⁶, most of this material ricochets out of the crater at high velocity, so that low impact angle itself does not enhance projectile contribution to the central peak: We do not expect to observe large amounts of projectile material in the central peaks of craters formed by fast, highly oblique (and therefore rare) impacts. On the other hand, moderately oblique impacts at low speed retain up to 50% of the projectile⁷. When a complex crater can form, our results show that this material becomes concentrated in the central peak area by the collapse flow.

The distribution of impact velocities on the Moon was evaluated from a numerical simulation of asteroid orbital evolution and the resulting impact velocities on the Moon^{24,25}. These simulations

¹State Key Laboratory of Remote Sensing Science, Institute of Remote Sensing Applications, Chinese Academy Sciences, Beijing, Beijing 100101, China,

²Department of Earth, Atmospheric and Planetary Sciences, Purdue University, West Lafayette, Indiana 47907, USA, ³Department of Physics, Purdue University, West Lafayette, Indiana 47907, USA. *e-mail: jmelosh@purdue.edu

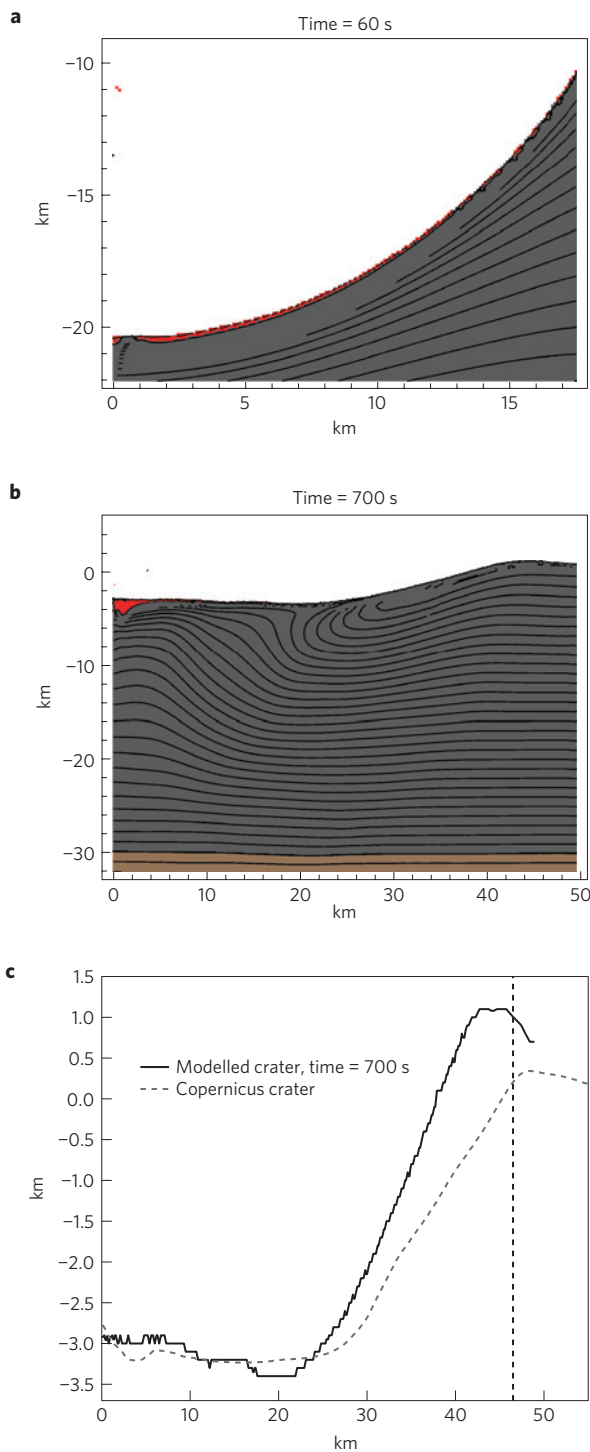


Figure 1 | Formation of Copernicus crater by a low-speed impact.

Copernicus crater following the impact of a 7-km-diameter dunite asteroid at 10 km s^{-1} . **a**, 60 s after initial impact, a thin layer of impactor material (red) lines the transient crater. **b**, 700 s after impact, the impactor material (red) is concentrated in the central peak of the crater. The maximum depth of excavation is 6–7 km. **c**, The final crater (solid black line) is 4.5 km deep, the central peak height is 0.5 km and the rim-to-rim diameter is ~ 89 km. The grey dashed line is from LOLA topography³⁰. Grey colour indicates crust and brown indicates mantle material.

show that about 25% of lunar impacts occur at speeds below 12 km s^{-1} , so that a significant fraction of lunar impactor material may remain largely intact in the central peaks of large lunar craters.

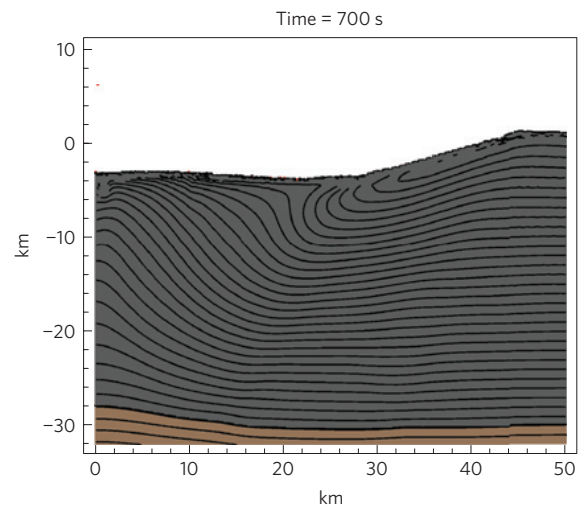


Figure 2 | Formation of Copernicus crater by a high-speed projectile.

Shown at 700 s after a 7-km-diameter dunite asteroid impacted at 14 km s^{-1} . Projectile material (red) has been almost completely vaporized leaving very little projectile material in the crater. The maximum depth of excavation is 6–7 km, shown by the originally horizontal black lines. This crater has a rim-to-rim diameter of 94 km, a rim-to-floor depth of 5.2 km, and a peak ring height of 0.95 km at a radius of 6 km.

To validate the results, we used a previously published simulation of the orbital evolution of the asteroids in the main belt²⁵ and derived the lunar impact velocity distribution as shown in Fig. 3. In this simulation the cumulative effects of weak resonances and perturbations from the major planets were the main cause of orbital drift and the diffusion of test bodies from the main belt region into the near-Earth asteroid (NEA) region. We cloned objects that were found to be on NEA-like orbits and integrated them as test particles using the MERCURY integrator with its hybrid symplectic algorithm capable of following particles through close encounters with planets²⁶. Particles that had a closest-approach distance within the Hill sphere of the Moon were considered to be potential projectiles. The impact velocity for a potential projectile was calculated from the projectile velocity relative to the Moon at closest approach, plus a contribution arising from the potential energy difference between the closest approach distance and the lunar surface that was calculated using the vis-viva equation. In our simulation there were 14,331 asteroid encounters and the percentage of impact velocities no higher than 12 km s^{-1} was about 25.1%, shown by the hatched area in Fig. 3. These numbers agree closely with those of another study²⁷, which were derived directly from a different dynamical model of the NEA population. We compare both distributions in the Supplementary Information.

The planetary geology community has not previously considered the possibility that large quantities of projectile material might remain intact in a large impact crater. Experience with terrestrial impact craters supports this view: except for small craters, in which the projectile is substantially slowed by atmospheric drag, traces of the projectile are difficult to find. At typical Earth impact velocities the projectile is largely vaporized or melted and thus mixes with a much larger volume of target material. Even on the Moon, the mean impact velocity is so high that, in most cases, the projectile melts or vaporizes. However, the minimum impact velocity on the Moon is its escape velocity, only 2.4 km s^{-1} and (owing to the vagaries of orbital encounters) a substantial fraction of impacts occur at much less than the mean velocity.

Even at lower impact velocities, the projectile is crushed and its fragments dispersed by the excavation flow. A recent paper²⁸ reports the discovery of small projectile fragments in lunar regolith samples,

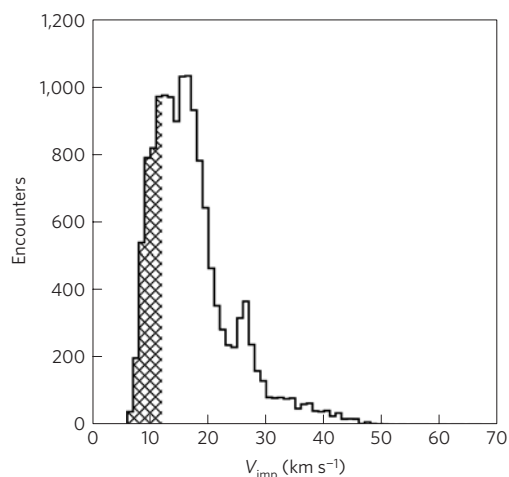


Figure 3 | Impact velocity distribution on the Moon. Based on 14,331 simulated asteroid impacts, the cross-hatched area represents events with impact velocity less than 12 km s^{-1} . The distribution is highly skewed, with mean and median values of 17.4 km s^{-1} and 15.9 km s^{-1} , respectively, and an r.m.s. value of 18.8 km s^{-1} .

consistent with dispersal in a low-velocity impact. However, as we have shown, the collapse of a crater to form a central peak reverses the excavation flow and tends to reassemble the dispersed projectile into a more coherent mass (although mixed with some amount of target material). It is thus, surprisingly, reasonable to expect to find a signature of the projectile in the central peak complex of craters on bodies whose gravitational acceleration is large enough to produce this type of crater.

The list of bodies that are neither too small nor too large to show a projectile signature is relatively short: the Moon, as we have argued here, as well as (marginally) Mars, with an escape velocity of 5.2 km s^{-1} and a large number of central peak craters. In addition, central peak craters occur on the icy satellites of the outer solar system. Although even low-velocity impacts may melt or vaporize ices in cometary impactors, some silicate signature may survive. Asteroids are generally too small to initiate crater collapse, with the notable exception of Rheasilvia crater on 4 Vesta. It is thus intriguing that the Dawn spectrometer has singled out the central peak of Rheasilvia as a unique feature on its surface²⁹. The Dawn team attributes this signature to deeper horizons excavated by the crater, but in view of the low impact velocities prevailing in the asteroid belt, the possibility of an impactor signature should not be ruled out.

Received 17 October 2012; accepted 17 April 2013;
published online 26 May 2013

References

- Evans, N. J., Gregoire, D. C., Grieve, R. A. F., Goodfellow, W. D. & Veizer, J. Use of platinum-group elements for impactor identification: Terrestrial impact craters and Cretaceous–Tertiary boundary. *Geochim. Cosmochim. Acta* **57**, 3737–3748 (1993).
- Tagle, R. & Hecht, L. Geochemical identification of projectiles in impact rocks. *Meteorit. Planet. Sci.* **41**, 1721–1735 (2006).
- Maier, W. D. *et al.* Discovery of a 25-cm asteroid clast in the giant Morokweng impact crater, South Africa. *Nature* **441**, 203–206 (2006).
- Kyte, F. T. A meteorite from the Cretaceous/Tertiary boundary. *Nature* **396**, 237–239 (1998).
- Pierazzo, E. & Chyba, C. F. Amino acid survival in large cometary impacts. *Meteorit. Planet. Sci.* **34**, 909–918 (1999).
- Pierazzo, E. & Melosh, H. J. Hydrocode modeling of oblique impacts: The fate of the projectile. *Meteorit. Planet. Sci.* **35**, 117–130 (2000).
- Bland, P. A. *et al.* Asteroids on the Moon: Projectile survival during low velocity impact *LPSC Conference*, XXXIX: Abs. #2045 (2008).
- Gross, J. & Treiman, A. H. Unique spinel-rich lithology in lunar meteorite ALHA 87005: Origin and possible connection to M^3 observations of the farside highlands. *J. Geophys. Res.* **116**, E10009 (2011).
- Pieters, C. *et al.* Mg-spinel lithology: A new rock type on the lunar farside. *J. Geophys. Res.* **116**, E00G08 (2011).
- Pieters, C. Conspicuous crater central peak: Lunar mountain of unique composition. *Science* **215**, 59–61 (1982).
- Yamamoto, S. *et al.* Possible mantle origin of olivine around lunar impact basins detected by SELENE. *Nature Geoscience* **3**, 533–536 (2010).
- Sunshine, J., Connolly, H. C., McCoy, T. J., Bus, S. J. & La Croix, L. M. Ancient asteroids enriched in refractory inclusions. *Science* **320**, 514–517 (2008).
- Brearley, A. J. & Jones, R. H. in *Planetary Materials, Rev. Mineral Vol. 36* (eds Papike, J. J. & Ribbe, P. H.) 1–398 (Mineral. Soc. Amer., 1998).
- Mittlefehldt, D. W., McCoy, T. J., Goodrich, C. A. & Kracher, A. in *Planetary Materials, Rev. Mineral Vol. 36* (eds Papike, J. J. & Ribbe, P. H.) 1–195 (Mineral. Soc. Amer., 1998).
- Burbine, T. H. & Binzel, R. P. Small main-belt asteroid spectroscopic survey in the near-infrared. *Icarus* **159**, 469–499 (2002).
- Dhingra, D. & Pieters, C. Mg-spinel rich lithology at crater Copernicus. *LPSC Conference*, XVII: Abs. #2024 (2011).
- Dhingra, D. *et al.* Compositional diversity at Theophilus crater: Understanding the geological context of Mg-spinel bearing central peaks. *Geophys. Res. Lett.* **38**, L11201 (2011).
- Kaur, P., Chauhan, P., Bhattacharya, S., Kiran, A. J. & Kumar, S. Compositional diversity at Tycho crater: Mg-spinel exposures detected from Moon Mineralogical Mapper (M^3) data. *LPSC Conference*, XLIII: Abs. #1434 (2012).
- Gagnepain-Beyneix, J., Lognonné, P., Chenet, H., Lombardi, D. & Spohn, T. A seismic model of the lunar mantle and constraints on temperature and mineralogy. *Phys. Earth Planet. Inter.* **159**, 140–166 (2006).
- Grieve, R. A. F., Robertson, P. B. & Dence, M. R. in *Multiring Basins* (eds Schultz, P. H. & Merrill, R. B.) 37–57 (Pergamon, 1981).
- Melosh, H. J. *Impact Cratering: A Geologic Process* (Oxford Univ. Press, 1989).
- Pierazzo, E. & Melosh, H. J. Understanding oblique impacts from experiments, observations and modeling. *Annu. Rev. Earth Planet. Sci.* **28**, 141–167 (2000).
- Eckholm, A. & Melosh, H. J. Crater features diagnostic of oblique impacts: The size and position of the central peak. *Geophys. Res. Lett.* **28**, 623–626 (2001).
- Bottke, W. F., Nolan, M. C., Melosh, H. J., Vickery, A. M. & Greenberg, R. Origin of the Spacewatch small Earth-approaching asteroids. *Icarus* **122**, 406–427 (1996).
- Minton, D. A. & Malhotra, R. A record of planet migration in the main asteroid belt. *Nature* **457**, 1109–1111 (2009).
- Chambers, J. E. A hybrid symplectic integrator that permits close encounters between massive bodies. *Mon. Not. R. Astron. Soc.* **304**, 793–799 (1999).
- Marchi, S., Mottola, S., Cremonese, G., Massironi, M. & Martellato, E. A new chronology for the Moon and Mercury. *Astrophys. J.* **137**, 4936–4948 (2009).
- Joy, K. H. *et al.* Direct detection of projectile relics from the end of the lunar basin-forming epoch. *Science* **336**, 1426–1429 (2012).
- De Sanctis, M. C. *et al.* Spectroscopic characterization of mineralogy and its diversity across Vesta. *Science* **336**, 697–700 (2012).
- Smith, D. E. *et al.* The lunar orbiter laser altimeter investigation on the lunar reconnaissance orbiter mission. *Space Science Rev.* **150**, 209–241 (2009).

Acknowledgements

We gratefully acknowledge the developers of iSALE2D, the simulation code used in our research, including G. Collins, K. Wünnemann, B. Ivanov and D. Elbeshausen. We thank B. Bottke for pointing out the further implications of Mg-spinel and helpful discussion. The research was supported by the National Natural Science Foundation of China (Grant No. 41002120 and 41171355) and NASA PGG grant NNX10AU88G.

Author contributions

Z.Y. conceived the research and implemented the Copernicus simulations with the help of B.C.J., who refined the hydrocode models to better fit the observations and created the crater profile from LOLA data; H.J.M. first realized the possibility that the olivine in Copernicus central peaks might be from the projectile; D.A.M. proved the presumption of low impact velocity on the lunar surface, and Z.Y. confirmed the similarity of mafic minerals between the central peaks and the asteroid. K.D., W.H. and Y.L. obtained and processed data used to support our research.

Additional information

Supplementary information is available in the online version of the paper. Reprints and permissions information is available online at www.nature.com/reprints. Correspondence and requests for materials should be addressed to H.J.M.

Competing financial interests

The authors declare no competing financial interests.